X-ray Absorption Study of PdCu Bimetallic Alloy Nanoparticles Containing an Average of ∼64 Atoms

Sue V. Myers,[†] Anatoly I. Frenkel,[*,‡] and Richard M. Crooks[*,†]

[†]*Department of Chemistry and Biochemistry, Texas Materials Institute, Center for Nano- and Molecular Science and Technology, The University of Texas at Austin, 1 University Station, A5300, Austin, Texas 78712-0165, and* [‡]*Department of Physics, Yeshiva University, 245 Lexington Avenue, New York, New York 10016*

The synthesis and characterization of PdCu bimetallic nanoparticles and Pd and Cu monometallic nanoparticles, consisting of an average of ∼64 atoms, is described. The bimetallic nanoparticles were prepared by cocomplexation of Pd^{2+} and Cu^{2+} to interior functional groups of a sixth-generation poly-(amidoamine) dendrimer template, followed by chemical reduction to yield dendrimer-encapsulated nanoparticles (DENs). Extended X-ray absorption fine structure (EXAFS) spectroscopy indicates that the particles have an alloy structure. TEM studies indicate particle diameters of 1.2−1.3 nm. This is a rare example of a stable nanoparticle in this size range that consists of one reactive metal and one substantially more noble metal. Such materials are predicted by first-principles theory to have interesting catalytic properties.

Introduction

Here we report the synthesis and characterization of PdCu bimetallic alloy nanoparticles consisting of an average of ∼64 atoms. Calculations have shown that such materials, composed of electron donor and acceptor metals, can exhibit desirable catalytic properties for the oxygen reduction reaction (ORR).[1−4] Specifically, when an electron donor atom, such as Cu, is present in the core and an electron acceptor, such as Pd, is present in the shell, then the d-band of the shell is lowered and its local electronic properties are predicted to be more like Pt. However, first-principles calculations are only available for particles containing small numbers of atoms (typically < ∼100). Accordingly, there is an urgent need to prepare well-defined, bimetallic nanoparticles in this size range that consist of both donor and acceptor elements.

The nanoparticles discussed here were prepared by cocomplexation of Pd^{2+} and Cu^{2+} to interior functional groups of a dendrimer template followed by chemical reduction to yield dendrimer-encapsulated nanoparticles (DENs).[5] Extended X-ray absorption fine structure (EXAFS) spectroscopy indicates that the particles have the expected alloy structure. Thus, although these materials are alloys rather than core/shell nanoparticles, we view the findings presented here as an important first step toward our eventual goal of

synthesizing and characterizing very well-defined nanoparticles whose electrocatalytic properties can be directly compared to theory.

The synthesis of metallic nanoparticles via dendrimer templating has previously been used by our group and others to prepare well-defined monometallic and bimetallic DENs consisting of Pt,[6−14] Cu,[15] Au,[16−20] Pd,[12,14,21−27]

(6) Lang, H.; May, R. A.; Iversen, B. L.; Chandler, B. D. *J. Am. Chem. Soc.* **2003,** *125,* 14832–14836.
(7) Alexeev, O. S.; Siani, A.; Lafaye, G.; Williams, C. T.; Ploehn, H. J.; Amiridis, M. D. *J. Phys. Chem. B* **2006,** *110,* 24903–24914.
(8) Ozturk, O.; Black, T. J.; Perrine, K.; Pizzolato, K.; Williams, C. T.; Parsons, F. W.; Ratliff, J. S.; Gao, J.; Murphy, C. J.; Xie, H.; Ploehn, H. J.; Chen, D. A. *Langmuir* **2005,** *21,* 3998–4006.
(9) Vijayaraghavan, G.; Stevenson, K. J. *Langmuir* **2007,** *23,* 5279–5282.
(10) Zhao, M.; Crooks, R. M. *Adv. Mater.* **1999,** *11,* 217–220.
(11) Esumi, K.; Nakamura, R.; Suzuki, A.; Torigoe, K. *Langmuir* **2000,** *16,* 7842–7846.
(12) Oh, S. K.; Kim, Y. G.; Ye, H.; Crooks, R. M. *Langmuir* **2003,** *19,* 10420–10425.
(13) Ye, H.; Crooks, R. M. *J. Am. Chem. Soc.* **2005,** *127,* 4930–4934.
(14) Ye, H.; Scott, R. W. J.; Crooks, R. M. *Langmuir* **2004,** *20,* 2915–2920.
(15) Zhao, M.; Sun, L.; Crooks, R. M. *J. Am. Chem. Soc.* **1998,** *120,* 4877–4878.
(16) Tran, M. L.; Zvyagin, A. V.; Plakhotnik, T. *Chem. Commun.* **2006,** 2400–2401.
(17) Gröhn, F.; Bauer, B. J.; Akpalu, Y. A.; Jackson, C. L.; Amis, E. J. *Macromolecules* **2000,** *33,* 6042–6050.
(18) Esumi, K.; Satoh, K.; Torigoe, K. *Langmuir* **2001,** *17,* 6860–6864.
(19) Gröhn, F.; Gu, X.; Grüll, H.; Meredith, J. C.; Nisato, G.; Bauer, B. J.; Karim, A.; Amis, E. J. *Macromolecules* **2002,** *35,* 4852–4854.
(20) Kim, Y. G.; Oh, S. K.; Crooks, R. M. *Chem. Mater.* **2004,** *16,* 167–172.
(21) Wilson, O. M.; Knecht, M. R.; Garcia-Martinez, J. C.; Crooks, R. M. *J. Am. Chem. Soc.* **2006,** *128,* 4510–4511.
(22) Chechik, V.; Crooks, R. M. *J. Am. Chem. Soc.* **2000,** *122,* 1243–1244.
(23) Yeung, L. K.; Crooks, R. M. *Nano Lett.* **2001,** *1,* 14–17.
(24) Ooe, M.; Murata, M.; Mizugaki, T.; Ebitani, K.; Kaneda, K. *Nano Lett.* **2002,** *2,* 999–1002.
(25) Niu, Y.; Crooks, R. M. *Chem. Mater.* **2003,** *15,* 3463–3467.

*To whom correspondence should be addressed. E-mail: anatoly.frenkel@yu.edu (A.I.F.); crooks@cm.utexas.edu (R.M.C.). Phone: 212-340-7827 (A.I.F.); 512-475-8674 (R.M.C.).

(1) Fernández, J. L.; White, J. M.; Sun, Y. M.; Tang, W. J.; Henkelman, G.; Bard, A. J. *Langmuir* **2006,** *22,* 10426–10431.
(2) Greeley, J.; Nørskov, J. K. *Surf. Sci.* **2005,** *592,* 104–111.
(3) Nilekar, A. U.; Xu, Y.; Zhang, J. L.; Vukmirovic, M. B.; Sasaki, K.; Adzic, R. R.; Mavrikakis, M. *Top. Catal.* **2007,** *46,* 276–284.
(4) Tang, W.; Henkelman, G. *J. Chem. Phys.* **2009,** *130,* 194504.
(5) Scott, R. W. J.; Wilson, O. M.; Crooks, R. M. *J. Phys. Chem. B* **2005,** *109,* 692–704.

PtPd,[28,29] PdRh,[30] PdAu,[5,31] PtCu,[32] and AuAg.[5] This technique has proven to be a powerful means for synthesizing nanoparticles containing less than 250 atoms and that are tailored to specific sizes and compositions not accessible by standard methods. Bimetallic particles can be engineered to have either a core−shell or alloy structure depending on the synthesis method used and the types of metals.

There has been one previous study of unsupported PdCu nanoparticles in the size range relevant to the present report. Specifically, Asakura and co-workers used EXAFS to characterize the structure of polymer-stabilized PdCu alloy nanoparticles dispersed in a glycol solution.[33] A preference for heterobond formation between the two metals was observed. There has also been one EXAFS study of supported PdCu bimetallic nanoparticles having diameters in the 2−6 nm range.[34] These materials were prepared by either an atomic layer epitaxy technique or by coimpregnation of the metals onto SiO_2 and γ-Al_2O_3 supports. The results indicated that the structure of the particles was dependent on the properties of the support: nanoparticles prepared on silica substrates had an alloyed structure whereas particles on alumina exhibited surface segregation of the Cu.

In the present study, Pd^{2+} and Cu^{2+} salts were added to a dilute solution of sixth-generation, hydroxyl-terminated poly(amidoamine)(PAMAM) dendrimers (G6-OH) at five different ratios of Pd^{2+}/Cu^{2+}. The total metal-ion-to-dendrimer content was fixed at 64:1, because this ratio represents the maximum loading of Cu^{2+} ions into the interior of G6-OH PAMAM dendrimers.[15] UV−vis absorption spectra indicate complete complexation of the metal salts to the dendrimer. The metal-ion/dendrimer precursor complex was reduced with BH_4^-, which yielded DENs having diameters in the range of 1.2−1.3 nm as measured by TEM. The coordination environments of the two metals were measured by EXAFS and fit those of an alloy structure. The particle size was also estimated from the EXAFS data and was found to be in good agreement with the TEM results.

Experimental Section

Chemicals. G6-OH dendrimers in methanol were purchased from Dendritech, Inc. (Midland, MI). The methanol was removed by vacuum evaporation at 23 ± 3 °C prior to use, and either a 100 or a 500 μM aqueous stock solution was prepared. K_2PdCl_4 and $NaBH_4$ were purchased from Sigma-Aldrich. $CuSO_4$ was purchased from Fisher Scientific. All chemicals were
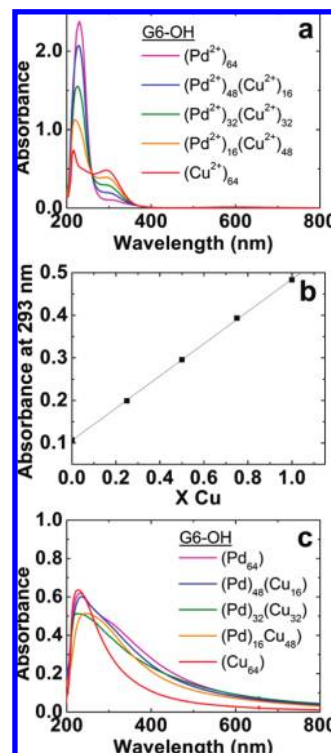
(26) Scott, R. W. J.; Ye, H.; Henriquez, R. R.; Crooks, R. M. *Chem. Mater.* **2003**, *15*, 3873–3878.
(27) Garcia-Martinez, J. C.; Lezutekong, R.; Crooks, R. M. *J. Am. Chem. Soc.* **2005**, *127*, 5097–5103.
(28) Ye, H.; Crooks, R. M. *J. Am. Chem. Soc.* **2007**, *129*, 3627–3633.
(29) Scott, R. W. J.; Datye, A. K.; Crooks, R. M. *J. Am. Chem. Soc.* **2003**, *125*, 3708–3709.
(30) Chung, Y.-M.; Rhee, H.-K. *J. Mol. Catal. A: Chem.* **2003**, *206*, 291–298.
(31) Knecht, M. R.; Weir, M. G.; Frenkel, A. I.; Crooks, R. M. *Chem. Mater.* **2008**, *20*, 1019–1028.
(32) Hoover, N. N.; Auten, B. J.; Chandler, B. D. *J. Phys. Chem. B* **2006**, *110*, 8606–8612.
(33) Bian, C. R.; Suzuki, S.; Asakura, K.; Ping, L.; Toshima, N. *J. Phys. Chem. B* **2002**, *106*, 8587–8598.
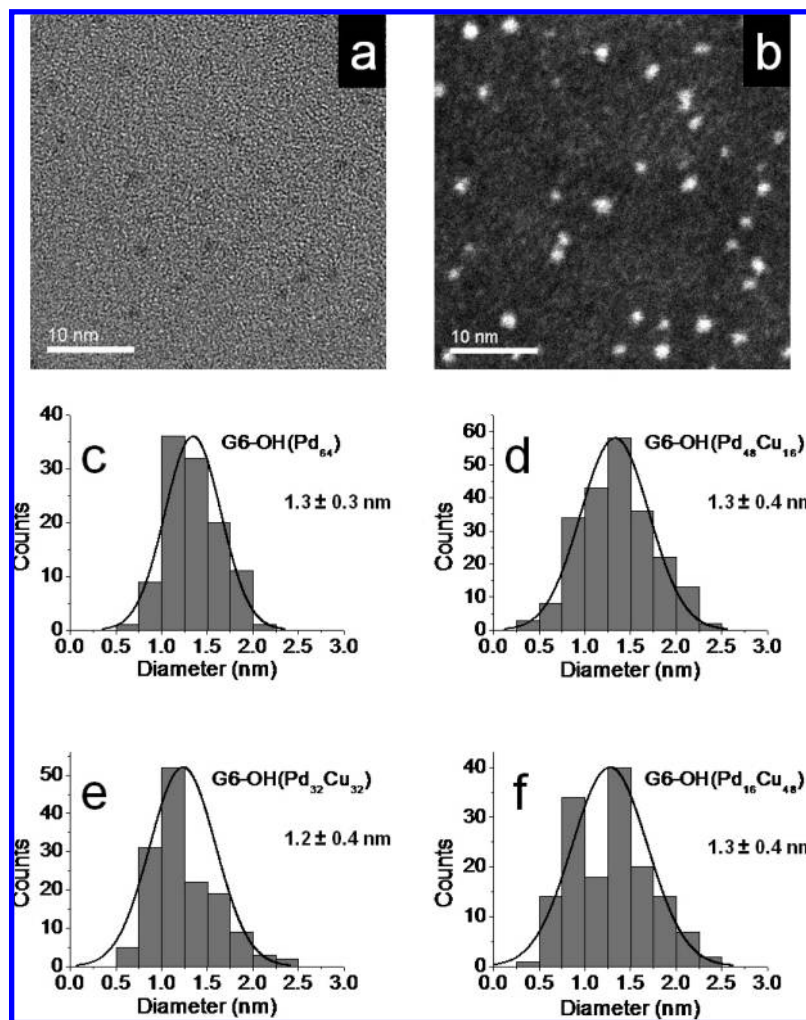(34) Molenbroek, A. M.; Haukka, S.; Clausen, B. S. *J. Phys. Chem. B* **1998**, *102*, 10680–10689.

Figure 1. (a) UV−vis absorption spectra for 2.0 μM G6-OH$(Pd^{2+})_x$-$(Cu^{2+})_{(64-x)}$ (x = 64, 48, 32, 16, 0) complexes. (b) Absorbance of G6-OH$(Pd^{2+})_x(Cu^{2+})_{(64-x)}$ complexes at λ_{max} for the Cu^{2+} LMCT peak. (c) Spectra of the G6-OH$(Pd^{2+})_x(Cu^{2+})_{(64-x)}$ complexes after reduction with BH_4^-. The optical path length of the cuvette was 1.00 cm. 2.0 μM G6-OH was used as the background.

used without further purification; 18 M$\Omega \cdot$cm Milli-Q deionized water was used to make all solutions.

Synthesis of DENs. Bimetallic DENs having different ratios of Pd/Cu are denoted as G6-OH$(Pd_xCu_{(64-x)})$ (x = 64, 48, 32, 16, 0). Note, however, that these nominal representations of DEN composition represent the average number of metal atoms in each DEN based upon the ratio of metal salts used to prepare the precursor complexes. Previous single-particle energy dispersive X-ray spectroscopy (EDS) studies of bimetallic DENs have demonstrated that the composition of individual particles is quite close to this ratio.[5,28] However, because of the difficulty of imaging PdCu DENs in the TEM used for EDS studies it was not possible to obtain reliable EDS data.

DENs were prepared by the following cocomplexation method.[5] A sufficient aliquot of 10.0 mM K_2PdCl_4 was added to an aqueous G6-OH solution to yield the desired Pd^{2+}/G6-OH ratio. This mixture was stirred for 10 min to permit complexation of Pd^{2+} to the interior tertiary amines of the dendrimer.[26] Next, sufficient 10.0 mM $CuSO_4$ was added to this solution to give the desired Pd^{2+}/Cu^{2+} ratio. This solution was stirred for 5 min, and then the pH was adjusted with NaOH to the optimal range for Pd^{2+} and Cu^{2+} complexation: between 7 and 8. The final dendrimer concentration was either 2 or 100 μM. The solution was bubbled with N_2 for a minimum of 10 min, and then 10 mol equiv of $NaBH_4$ (relative to the total metal content) was added to the solution.

Characterization. UV−vis absorbance spectra were obtained using a Hewlett-Packard HP8453 spectrometer and a 1.00 cm path length quartz cuvette. A solution of G6-OH in water was used for background correction.

TEM images were collected using a JEOL-2010F TEM operating at 200 kV. Images were collected in transmission, as

Figure 2. (a) Bright-field TEM micrograph and (b) HAADF STEM micrograph for G6-OH(Pd$_{32}$Cu$_{32}$). Particle size distribution for (c) Pd monometallic and (d−f) PdCu bimetallic DENs.

well as high-angle annular dark field (HAADF) mode. TEM grids were prepared by dropping several microliters of a 2 μM DEN solution onto a carbon-coated 400-mesh Cu grid (EM Sciences) and drying in air.

EXAFS data were collected on beamline X18b at the National Synchrotron Light Source at the Brookhaven National Laboratory in New York; 100 μM solutions of freshly reduced DENs were placed in 1 cm thick solution cells having Kapton tape windows. The K absorption edges of Pd and Cu were measured simultaneously in transmission and fluorescence modes, by orienting the sample 45 degrees relative to the beam. A five-grid Lytle detector filled with Ar gas was used for fluorescence detection, and in the case of the Cu K-edge, Soller slits and a Ni filter were used. At least two and as many as eight, energy scans were averaged to improve the signal-to-noise ratio. Pd and Cu foil reference spectra were collected concurrently with the DENs spectra at the Pd and Cu K-edge, respectively, and were used for energy calibration. The data were analyzed using the IFEFFIT software package and FEFF6 program.[35,36] The details of our data modeling procedure for monometallic and bimetallic systems are presented below.

Results and Discussion

UV−vis Analysis of Cu, Pd, and PdCu DENs. Figure 1a shows UV−vis absorption spectra of 2.0 μM aqueous solutions of G6-OH(Pd^{2+})$_x$(Cu^{2+})$_{64-x}$ (x = 64, 48, 32, 16, 0) before reduction with BH$_4{}^-$. The DEN precursor solutions exhibit strong absorption bands at ∼230 and 290 nm and an isosbestic point at 261 nm. These peaks arise from ligand-to-metal charge-transfer (LMCT) bands associated with the dendrimer/metal-ion complexes.[15,26] Pd^{2+} salts not associated with the dendrimer absorb in this region, and therefore, the presence of an isosbestic point implies that all of the Pd^{2+} salts have complexed to the dendrimer interior. The absorbance data for G6-OH(Cu^{2+})$_{64}$ and G6-OH(Pd^{2+})$_{64}$ are comparable to previously published results.[15,26]

The optimal pH range for complexation of the metal salts to the dendrimer was found to be between 7 and 8. Complexation of Cu^{2+} is pH dependent due to competition of H$^+$ for binding sites at low pH.[37,38] At high pH

(35) Ravel, B.; Newville, M. *J. Synchrotron Rad.* **2005**, *12*, 537–541.
(36) Zabinsky, S. I.; Rehr, J. J.; Ankudinov, A.; Albers, R. C.; Eller, M. J. *Phys. Rev. B* **1995**, *52*, 2995.

(37) Diallo, M. S.; Christie, S.; Swaminathan, P.; Balogh, L.; Shi, X.; Um, W.; Papelis, C.; Goddard, W. A.; Johnson, J. H. *Langmuir* **2004**, *20*, 2640–2651.
(38) Wan, H.; Li, S.; Konovalova, T. A.; Shuler, S. F.; Dixon, D. A.; Street, S. C. *J. Phys. Chem. C* **2008**, *112*, 1335–1344.
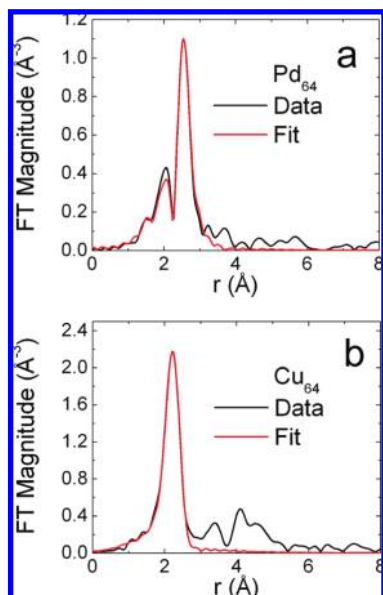
Figure 3. EXAFS data (black) and simulated fits (red) for (a) G6-OH-(Pd$_{64}$) and (b) G6-OH(Cu$_{64}$).

Table 1. Fitting Parameters for PdCu DENs

G6-OH	n_{ind}[a]	n_{var}[b]	k-range (Å^{-1}) Pd	k-range (Å^{-1}) Cu	r-range Pd	r-range Cu
Cu$_{64}$	14	4		2−14		1−2.8
Pd$_{16}$Cu$_{48}$	20	14	2−11	2−13	1.2−2.9	1.5−3
Pd$_{32}$Cu$_{32}$	21	14	2−12	3−12	1.2−2.9	1.1−3
Pd$_{48}$Cu$_{16}$	20	14	2−12	2−10	1.3−2.9	1−3
Pd$_{64}$	13	7	2−14		1.3−3	

[a] Number of independent data points. [b] Number of fit variables.

Table 2. First-Shell Coordination Numbers for PdCu DENs

G6-OH	n_{CuCu}	n_{CuPd}	n_{PdPd}	n_{PdE}
Cu$_{64}$	7.1 ± 0.4			
Pd$_{16}$Cu$_{48}$	4.2 ± 0.8	1.3 ± 0.4	3.5 ± 2.0	1.9 ± 0.9
Pd$_{32}$Cu$_{32}$	3.0 ± 1.1	3.1 ± 0.5	4.1 ± 1.3	0.8 ± 0.4
Pd$_{48}$Cu$_{16}$	0.9 ± 0.7	4.8 ± 1.9	4.0 ± 1.4	1.4 ± 0.5
Pd$_{64}$			6.5 ± 0.4	0.2 ± 0.2

values, loss of Pd from the complex is observed. In the pH range used for this study, the absorbances of the LMCT bands of the bimetallic precursors are proportional to the mole ratios of Pd^{2+} and Cu^{2+} present in the dendrimers (Figure 1b). This finding provides additional evidence that the metal ions completely bind to the dendrimer.

Following chemical reduction of the G6−OH(Pd^{2+})$_x$-(Cu^{2+})$_{64-x}$ complexes, the LMCT bands are replaced by broad, monotonically decreasing bands (Figure 1c) characteristic of interband transitions of spherical metal nanoparticles.[39] The irregular behavior below 230 nm is caused by the high absorbance of the dendrimer in this region. The absence of a plasmon at 570 nm in the monometallic copper sample indicates a particle diameter below 3 nm,[40] because damping of plasmon absorption bands is observed when particle sizes are smaller than the mean free path of conduction electrons in the absorbing metal.[39] It is not clear why the spectra do not exhibit a consistent trend as a function of particle composition, but this observation may reflect the fact that these alloys have unique optical properties that are not a simple sum of the properties of the component metals.

If the DENs are stored in a reducing atmosphere, such as a H$_2$-saturated aqueous solution, they are stable and their absorbance spectra do not change as a function of time. However, nonreducing environments, like air-saturated water, result in partial DEN oxidation and gradual regrowth of the LMCT bands. This observation is consistent with previous studies, although the exact mechanism of oxidation is not fully understood. Dry Pd DENs are stable in the presence of air, but Cu DENs oxidize in air even when dry.

TEM Analysis of Pd and PdCu DENs. The small size of these ∼64-atom PdCu DENS, in conjunction with the low

mass of Cu, make it difficult to obtain high-quality, bright-field TEM images. Therefore, particle diameters were estimated from HAADF-STEM micrographs. Due to their instability in air, it was not possible to obtain TEM images of Cu monometallic DENs. Figure 2a and b shows representative TEM images of the G6−OH-(Pd$_{32}$Cu$_{32}$) particles. Theoretical particle sizes are estimated to be 1.4 and 1.3 nm for monometallic Pd and Cu particles, respectively, assuming a spherical geometry. Histograms of the measured particle diameters are provided in Figure 2c−f, and they indicate that the measured particle diameters are just slightly smaller (1.2−1.3 nm).

EXAFS Fitting Procedure. The fits were constrained to include only the first coordination shells. This eliminates all multiple scattering effects and significantly reduces the number of independent variables. S_0^2 values were taken from fits to Pd and Cu reference foil data collected under similar conditions on beamline X18b. A k-weight of 2 was used for all fits.

Metal−metal (M−M) and metal−low Z (M−E, E = C, O, N) interactions were included in the preliminary simulations. Cu−E interactions were found to be well below the uncertainty of the fit, and therefore, they were not included in the final models for the Cu edge of the monometallic and bimetallic DENs. The CNs for Pd−E (n_{PdE}) are close to the uncertainty level of the fits for all DENs studied, but better fit values consistently resulted when Pd−E interactions were included. Further studies would be required to meaningfully quantify low-Z coordination to Pd.

The data from both metal edges of the bimetallic materials were fit simultaneously. The Pd−Cu (n_{PdCu}) and the Cu−Pd CNs (n_{CuPd}) were fixed according to eq 1,[41]

$$n_{PdCu} = \frac{\chi Cu}{\chi Pd} n_{CuPd} \qquad (1)$$

The heterometallic bond lengths and Debye−Waller factors were also constrained to be the same as measured from each edge (Pd or Cu).

(39) Creighton, J. A.; Eadon, D. G. *J. Chem. Soc., Faraday Trans.* **1991**, *87*, 3881–3891.
(40) Pileni, M. P.; Lisiecki, I. *Colloids Surf., A* **1993**, *80*, 63–68.

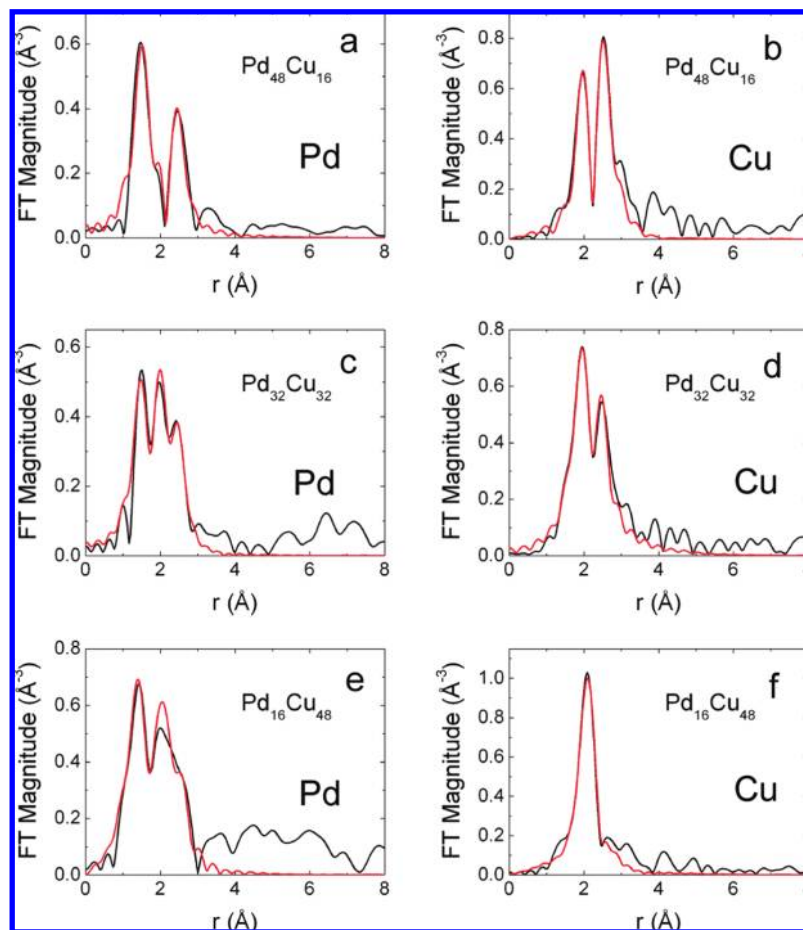(41) Via, G. H.; Drake, K. F.; Meitzner, G.; Lytle, F. W.; Sinfelt, J. H. *Catal. Lett.* **1990**, *5*, 25–33.

Figure 4. EXAFS data and fit results for the (a) Pd K edge and (b) Cu K edge of G6-OH(Pd$_{48}$Cu$_{16}$), (c) Pd K edge and (d) Cu K edge of G6-OH(Pd$_{32}$Cu$_{32}$), and (e) Pd K edge and (f) Cu K edge for G6-OH(Pd$_{16}$Cu$_{48}$). The data are plotted in black and the simulated fits are in red.

EXAFS Analysis of Monometallic Pd and Cu DENs. As discussed earlier, G6-OH(Pd$_x$Cu$_{(64-x)}$) DENs are only stable in reducing environments. Therefore, to prevent oxidation of the DENs during EXAFS experiments, the precursor complexes were reduced with NaBH$_4$ immediately prior to data collection. In addition to reducing the precursor ions to DENs, NaBH$_4$ also slowly reduces water to H$_2$. The presence of H$_2$ in the DEN solutions throughout the period required to obtain EXAFS spectra, as evidenced by continuous bubble formation, ensured the integrity of the DENs. Indeed, UV−vis spectroscopy experiments carried out under nearly identical conditions to those used at the beamline confirmed that no regrowth of the LMCT bands occurred. More significantly, the EXAFS analysis, discussed later, indicates minimal oxide formation under these conditions.

Because the samples are maintained in a reducing environment, Pd hydride formation is possible. The Pd−Pd bond lengths were measured at 2.78 Å, a 1.1% expansion over the bulk value for metallic Pd. This is consistent with the formation of the hydride in particles of this size.[42] However, the bimetallic nanoparticles did not exhibit this behavior (Table S1, Supporting Information).

Figure 3 shows the measured EXAFS data for the monometallic Pd and Cu DENs and theoretical fits of the first nearest neighbor contributions. The selected k-ranges and r-ranges for each edge as well as the number of variables from each fit are given in Table 1. The coordination numbers (CNs) obtained from the fits, together with their 95% confidence limits (error bars) are presented in Table 2.

The total metal−metal CN (n_{MM}) can be used to estimate the size of DENs, because as particle size decreases the ratio of low-coordination surface atoms to interior atoms increases and therefore the total metal−metal coordination decreases. Such method can be used only if independent information about the particle shape is available, as in our case, where it is known that the particles are quasi-spherical. The cuboctahedron cluster family was chosen to model CNs, because the values can be easily calculated for different cluster orders.[43−46]

The Pd and Cu monometallic DENs have n_{MM} values of 6.5 ± 0.4 and 7.1 ± 0.4, respectively. The theoretical fcc cuboctahedron first shell n_{MM} values for 13-, 55-, and

(42) Tew, M. W.; Miller, J. T.; van Bokhoven, J. A. *J. Phys. Chem. C* **2009**, *113*, 15140–15147.

(43) Montejano-Carrizales, J. M.; Aguilera-Granja, F.; Morán-López, J. L. *Nanostruct. Mater.* **1997**, *8*, 269–287.
(44) Frenkel, A. I. *J. Synchrotron Radiat.* **1999**, *6*, 293–295.
(45) Frenkel, A. I.; Hills, C. W.; Nuzzo, R. G. *J. Phys. Chem. B* **2001**, *105*, 12689–12703.
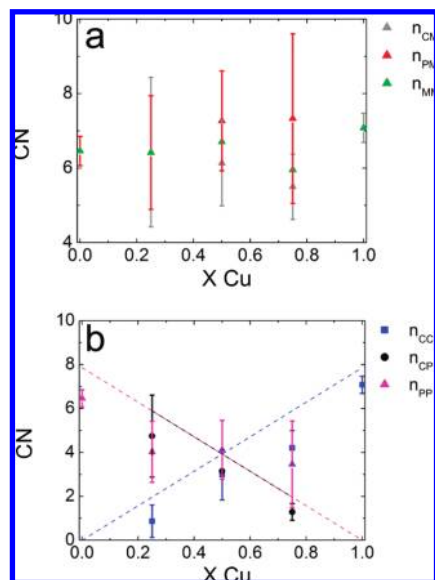(46) Frenkel, A. I. *Z. Krystallogr.* **2007**, *222*, 605–611.

Figure 5. (a) Pd−M, Cu−M, and M−M CN as a function of Cu composition. (b) Cu−Cu, Cu−Pd, and Pd−Pd coordination numbers as a function of Cu composition. The theoretical values for a 55 atom random alloy are indicated by dashed lines.

147-atom particles are 5.54, 7.86, and 8.98, respectively. Larger particles will have a CN approaching the bulk value of 12. Predicting a theoretical CN for a 64-atom particle is more difficult, because it does not have a complete outer shell. However, in certain situations (e.g., when the atoms forming an incomplete shell preferentially reside in the lower coordinated sites like vertices and edges) the CN of non-closed-shell clusters may decrease compared to that of the smaller closed-shell clusters. Such a scenario is required for the sizes of the monometallic DENs, as judged from the CNs, to be consistent with the TEM data and calculated values.

EXAFS Analysis of Bimetallic G6-OH(Pd$_x$Cu$_{(64-x)}$) DENs. As discussed in detail in a previous paper, the CNs for each metal in small, bimetallic particles can yield information about the structure of the material.[31] For example, if metal atoms of type A segregate to the interior of a particle containing atom types A and B, the coordination number n_{AM} of neighboring atoms to A will be larger than n_{BM} since the majority of atoms on or near the particle surface are of the type B, which see fewer neighbors, on the average, than A. The distribution of CNs obtained for all types (AM and BM) of interactions between the two metals can reveal core−shell structure (when the n_{AM} and n_{BM} are different) or the homogeneous alloy structure (when they are similar, within the uncertainties). Finally, for a bimetallic material, the CN n_{AB} that quantifies the coordination of atoms A by atoms B will increase with increased alloying of the two metals.

The EXAFS data and simulated results for the bimetallic DENs are shown in Figure 4. The CNs obtained from the fits are also given in Table 2. The data indicate that the two metals in the bimetallic DENs are mostly alloyed. As shown in Figure 5a, the Pd−M CN is the same or slightly higher than that of the Cu−M CN for all three

DEN compositions. However, if the DENs were to have a true Pd-core/Cu-shell structure, the Pd−M CN would be predicted to have a much higher value (> 10.7) in the G6-OH(Pd$_{16}$Cu$_{48}$) DENs. In this instance, nearly all of the 16 Pd atoms would be within the interior of the particle. Likewise, in Cu-core/Pd-shell material, the Cu−M CN of the G6-OH(Pd$_{48}$Cu$_{16}$) DENs would have a similarly high value.

The trends in the Cu−Cu and Cu−Pd CNs agree very well with the ideal alloy model (Figure 5b). The Pd−Pd CNs are slightly higher, especially for the G6-OH-(Pd$_{16}$Cu$_{48}$) DENs. This difference, however, falls within the uncertainty of the fits. Accordingly, it is not possible to distinguish a completely random and homogeneous alloy from an alloy having either a Pd- or Cu-rich core.

Summary and Conclusions

We have reported on the synthesis and characterization of Pd and Cu monometallic and PdCu bimetallic nanoparticles prepared within G6-OH dendrimer templates. Bimetallic nanoparticles, such as those described here, are predicted by theory to have desirable catalytic properties.[4] The UV−vis, TEM, and EXAFS data for these PdCu DENs are consistent with their size corresponding to an average of ∼64 atoms. Moreover, for the bimetallic DENs, the results indicate at least partial alloying of the two metals although the degree of alloying cannot be determined.

The ability to synthesize and characterize nearly monodisperse and fully stable particles in this size regime is important to our larger goal of correlating the size, composition, and structure of DENs to their catalytic function. Specifically, we are presently studying the kinetics of the electrochemical oxygen reduction reaction using these bimetallic PdCu DENs as electrocatalysts. These experimental results will be correlated to first-principles theory, with a view toward unification of theory and experiment. The results of that work will be reported in due course.

Supporting Information Available: Parameters from the fits of the EXAFS data (PDF). This material is available free of charge via the Internet at http://pubs.acs.org.